International Conference on Applied Energy 2019
Aug 12-15, 2019, Västerås, Sweden
Paper ID:937

NUMERICAL INVESTIGATIONS ON HEAT TRANSFER AND RESISTANCE PERFORMANCE OF OVAL-TUBE RECUPERATOR

Wenying Ye, Guo-Yan Zhou, Shan-Tung Tu, Xialing Hou

Key Laboratory of Pressure Systems and Safety (MOE), School of Mechanical and Power Engineering, East China University of Science and Technology, Shanghai 200237, PR China

ABSTRACT

An oval-tube structure is used as the new generation aero-engine recuperator, which has a wide range of application prospects in aerospace, marine and other important industrial fields. The heat transfer performance of this structure directly determines the energy efficiency of the aero engine. However, the enhanced heat transfer mechanism of oval-tube recuperator is not clear due to the lack of internal flow field information. Based on the standard *k-ε* model, shell-side heat transfer and resistance performance are conducted by using commercial CFD software FLUENT. The influences of structural parameters and tube arrangement on heat transfer and resistance performance are further studied. Then the mechanism on heat transfer augmentation is discussed according to the fluid flow characteristics and the field coordination principle. The results show that the standard *k-ε* and periodicity model is feasible and accurate to simulate the fluid flow on shell side of oval-tube recuperator. The heat transfer and resistance performance increase with the ratio of major and minor axes and longitudinal spacing of oval-tube. With the increase of horizontal and longitudinal spacing of oval-tube, the performance increases at first and then decreases. The maximum velocity appears at the minor axis, and the minimum value of fluid temperature, velocity and pressure appears at the major axis. The amplitude of field synergy angle is small in the inlet section, but the fluctuation amplitude in the recuperator is large.

Keywords: oval tube; recuperator; heat transfer; numerical simulation; computational fluid dynamics(CFD)

NONMENCLATURE

Abbreviations	
APEN	Applied Energy
Symbols	
n	Year

1. INTRODUCTION

Oval-tube recuperator is the most new type of recuperator used in aero-engine at present[1]. It has the advantages of compact structure and high heat transfer efficiency[2]. It can be used in the worse thermal cycle of gas turbine and has a high application prospect[3]. However, the recuperator is the subsidiary structure of the engine, adding the recuperator into the engine will make the total proportion of the engine high, which will affect the actual use effect, so it is necessary to study the heat transfer and resistance performance of the recuperator. The mechanism of heat transfer enhancement is discussed, which lays a foundation for the further optimization design of the recuperator.

At present, the performance of heat transfer and resistance of oval-tube recuperator is mainly studied in two aspects: experimental study and numerical simulation. The experimental research method can well measure the overall pressure and temperature change of the recuperator, but can not obtain the detailed distribution of the internal velocity, temperature and pressure of the recuperator. The numerical simulation method can be used to simulate the flow situation of the recuperator under complex working conditions, and the flow field distribution in the recuperator can be obtained. The numerical simulation of the heat transfer performance of aeroengine heat recuperator was studied by Kristikos and others by means of computational fluid dynamics(CFD)[4]. Kyprianidis et al studied the effect of turbulence intensity on pressure drop and heat transfer of recuperator by means of computational fluid dynamics. The results show that increasing turbulence intensity is helpful to reduce pressure drop and enhance heat transfer efficiency of recuperator[5]. Bouris et al. has carried on the numerical calculation to the heat transfer mechanism of the heat transfer tube in the recuperator, and has drawn the conclusion that the use of the oval-tube increases the heat transfer rate, because the lower pressure drop caused by the shape of the tube makes the tube can be placed on the closer spacing[6].

Previous scholars mainly used porous media model to pre-define the overall heat transfer and pressure drop behavior of the oval-tube recuperator. However, the flow distribution of the fluid in the recuperator can not be clearly reflected by using the porous media model. In this study, the periodic model of shell side of oval-tube recuperator is established, and the numerical simulation is carried out by using commercial fluid software FLUENT.

2. NUMERICAL MODEL

2.1 Geometrical model

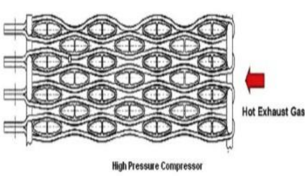

(a) Cross section diagram

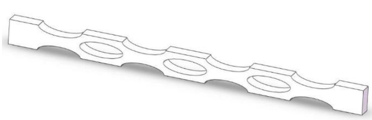

(b) Model diagram

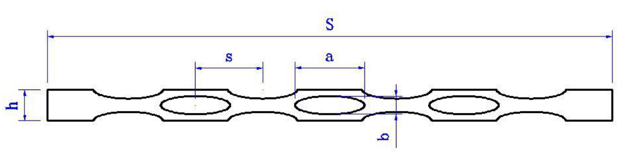

(c) A schematic diagram of the cross section size

Fig. 1 Model of oval tube recuperator

The overall model of the double-U oval-tube recuperator used in aero-engines is shown in Fig. 1(a) and (b) is a schematic diagram of the cross-section of an oval tube recuperator consisting of multiple oval-tubes 4-3-4 arrangement. Considering the symmetry and repeatability of the structure of the recuperator, the repeated section is taken as the research object of numerical calculation, and the concrete calculation model is shown in Fig. 1(c). The calculation model in this paper is a three-dimensional model of repeated segments, and the corresponding structural dimensions are shown in Table 1.

Table 1 Geometric parameters of the oval tube recuperator

Parameter	Values
Oval-tube long-axis a/mm	6.00
Oval-tube short-axis b/mm	1.56
Transverse tube spacing s/mm	5.52
Longitudinal tube spacing h/mm	2.70
Overall length S/mm	58.8

2.2 *Govening equation*

The flow of fluid in the shell side of the recuperator is turbulent motion, so in this paper, the Standard *k-ε* turbulence model is used to simulate the shell side of the aero-engine recuperator. The fluid in the shell side of the recuperator is a single-phase continuous fluid, which should satisfy the following governing equations.

Continuity equation:

$$\frac{\partial}{\partial x_i}(\rho u_i) = 0 \tag{1}$$

Momentum equation:

$$\frac{\partial}{\partial x_i}(\rho u_i u_k) = \frac{\partial}{\partial x_i}\left(\mu \frac{\partial u_k}{\partial x_i}\right) - \frac{\partial p}{\partial x_k} \tag{2}$$

Energy equation:

$$\frac{\partial}{\partial x_i}(\rho u_i t) = \frac{\partial}{\partial x_i}\left(\frac{k}{C_p}\frac{\partial t}{\partial x_i}\right) \tag{3}$$

Turbulent kinetic energy k equation:

$$\frac{\partial}{\partial t}(\rho k) + \frac{\partial}{\partial x_i}(\rho k u_i) = \frac{\partial}{\partial x_j}\left(\alpha_k \mu_{eff}\frac{\partial k}{\partial x_j}\right) + G_k + \rho\varepsilon \tag{4}$$

Turbulent dissipation rate ε equation:

$$\frac{\partial}{\partial t}(\rho\varepsilon) + \frac{\partial}{\partial x_i}(\rho\varepsilon u_i) = \frac{\partial}{\partial x_j}\left(\alpha_k \mu_{eff}\frac{\partial \varepsilon}{\partial x_j}\right) + C_{1\varepsilon}^{*}\frac{\varepsilon}{k}G_k - C_{2\varepsilon}\rho\frac{\varepsilon^2}{k} \tag{5}$$

where

$$\mu_{eff} = \mu + \mu_t, \quad \mu_t = \rho c_\mu \frac{k^2}{\varepsilon}, \quad C_{1\varepsilon}^{*} = C_{1\varepsilon} - \frac{\eta(1-\eta/\eta_o)}{1+\beta\eta^3},$$

$$\eta = \left(2E_{ij}\cdot E_{ij}\right)^{1/2}\frac{k}{\varepsilon}, \quad E_{ij} = \frac{1}{2}\left[\frac{\partial u_i}{\partial x_j} + \frac{\partial u_j}{\partial x_i}\right]$$

The parameters in the turbulence model are empirical. At the same time, the standard wall function is used to simulate the flow near the wall, and the dimensionless distance y^+ ranges from 10 to 100.

2.2 Boundary conditions and computational methodology

Considering the characteristics of the recuperator structure and the application range of the numerical calculation, the boundary conditions are simplified as appropriate:

(1) Inlet boundary: using velocity inlet boundary condition, given mean velocity, inlet temperature T_{in}=944K and turbulence intensity I =7%;

(2) Outlet boundary: assuming fully developed flow, free-flow outlet is used as a boundary condition;

(3) Wall conditions: the wall of heat exchanger is static and non-slip wall condition, the wall of heat exchanger is constant temperature, T_w=722K.

The medium of numerical calculation is air, and its physical properties are calculated according to piecewise-linear interpolation method at each temperature point. ANSYS FLUENT, is used to discretize the governing equations by using finite volume method, SIMPLE algorithm is used for the coupling of pressure and velocity, standard scheme is used for discretization of pressure terms[7], and second-order upwind scheme is used for other terms. The standard wall function method is used to treat the wall.

2.3 Mesh Generating and grid independence verification

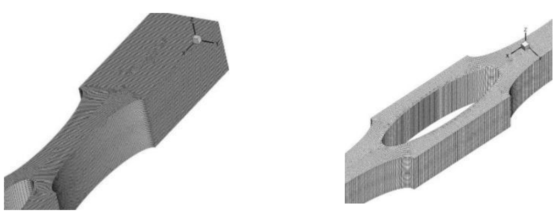

Fig. 2 Sketch of the grid system

Sketch of the grid system can be found in Fig. 2. The whole model was meshed with nonuniform unstructured grid with tetrahedron and face mesh was swept along the domain to discrete the whole volume of the recuperator. Considering about the efficiency and the accuracy of the simulation, the grid independence test has been done. The meshing scheme with the girds number of 1.39×10^6 employed in the present study.

2.4 Model verification

2.4.1 Turbulence model verification

In order to verify the accuracy of turbulence model, different turbulence models including Standard k–ε model, RNG k–ε model and Realized k–ε model are applied firstly. The simulation pressure drops are compared with the experimental results from the literature[8] as shown in Fig. 3. The results from Standard k–ε model are much closer to the experimental results when compared with other models. It can be concluded that the employment of the Standard k–ε model in this numerical study is reasonable.

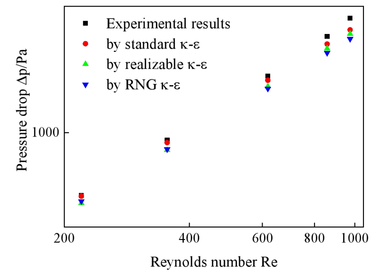

Fig. 3 Differences between the numerical and experimental results

2.4.2 Periodic model verification

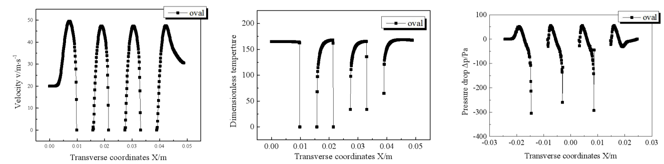

(a) Velocity (b) Temperture (c) Pressure drop

Fig. 4 Flow distribution on the central line of the cross section of an oval-tube recuperator

Fig. 4 shows that the velocity, temperature and pressure drop of the fluid in the flow field are periodically distributed, and the fluctuating peaks are basically the same. It can be concluded that the periodic model is feasible and accurate to describe the characteristics of fluid flow in this type of recuperator.

3. RESULTS AND DISCUSSIONS

3.1 Heat transfer and resistance performance

Fig. 5 shows the numerical results of heat transfer and pressure drop. The Nusselt number and the pressure drop of the shell side of the oval-tube recuperator increase with the increase of the Reynolds number, and the increasing extent of the pressure drop increases with the increase of the Reynolds number.

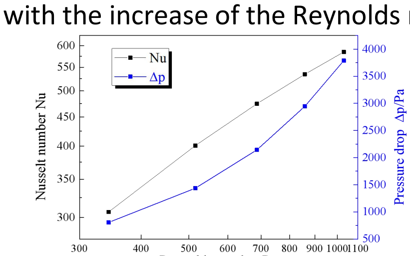

Fig.5 Heat transfer and resistance performance

3.2 I*nfluence of structural parameters and tube arrangement*

3.2.1 Influence of structural parameters

Six different structural dimensions are selected to change the long and short axis of the oval-tube, so that the cross section area of the oval-tube of the six kinds of oval-tube recuperator is the same, and the overall length and width of the model are the same, and its corresponding structure is shown in Table 2.

Table 2 Geometrical parameters of all models

	a/mm	*b*/mm	*a*/*b*	*s*/mm	*h*/mm	*S*/mm
case 1	5.50	1.70	3.23	5.8	2.7	48.8
case 2	5.64	1.66	3.40	5.8	2.7	48.8
case 3	5.85	1.60	3.66	5.8	2.7	48.8
case 4	6.00	1.56	3.85	5.8	2.7	48.8
case 5	6.24	1.50	4.16	5.8	2.7	48.8
case 6	6.50	1.44	4.51	5.8	2.7	48.8

Under the condition of the same tube spacing, the numerical results of heat transfer and pressure drop of six different oval-tube long and short axis recuperators are shown in Fig. 6. The comprehensive performance of recuperator increases gradually with the increase of the ratio of long to short axis of oval-tube.

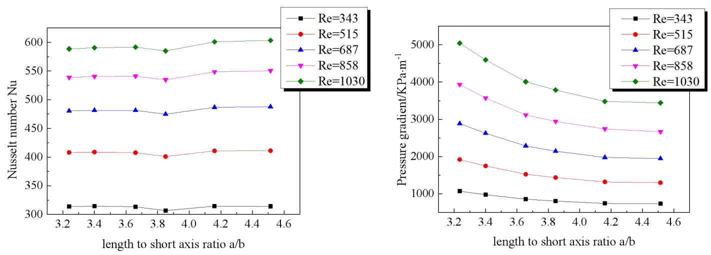

(a) Nusselt number (b) Pressure gradient

Fig.6 Effects of structural parameters on the heat transfer and pressure drop performance

3.2.2 Influence of tube arrangement mode

In order to study the heat transfer and pressure drop performance of different tube spacing heat recuperator, ten different models are selected, *a*=6mm, *b*=1.56mm, *S*=48.8mm, *s* and *h* are shown in Table 3.

Table 3 Geometrical parameters of all models

	case 7	case 8	case 9	case 10	case 11	case 12	case 13	case 14	case 15	case 16
s/mm	5.8	6.0	6.2	6.4	6.6	6.8	6.4	6.4	6.4	6.4
h/mm	2.7	2.7	2.7	2.7	2.7	2.7	2.1	2.3	2.5	2.9

Under the condition that the size of oval-tube is the same, the numerical results of heat transfer and pressure drop of five kinds of oval-tube with different transverse spacing of case7-case12, are simulated and calculated as shown in Fig. 7.

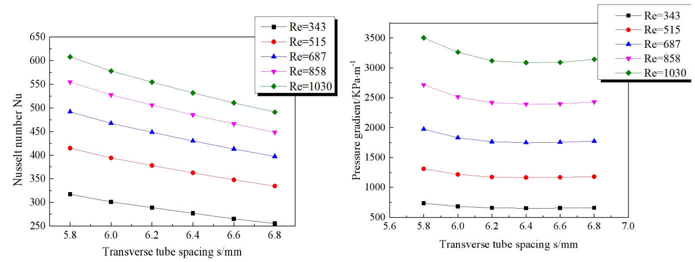

(a) Nusselt number (b) Pressure gradient

Fig.7 Influence by transverse tube spacing the heat transfer and pressure drop performance

With the increase of the transverse tube spacing of the oval-tube, the comprehensive performance of the recuperator increases at first and then decreases. When the Reynolds number is the same and the transverse tube spacing of the oval-tube is 6.4mm, the comprehensive performance of the recuperator is the best.

Under the condition of the same tube spacing, case 10, case 13-case 16, are simulated and calculated. The numerical results of heat transfer and pressure drop for five kinds of oval-tubes with different longitudinal spacing are shown in Fig. 8

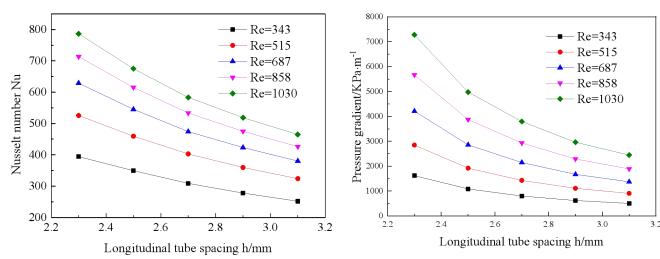

(a) Nusselt number (b) Pressure gradient

Fig. 8 Influence by longitudinal tube spacing the heat transfer and pressure drop performance

With the increase of the longitudinal tube spacing of the oval-tube, the comprehensive performance of the recuperator is gradually improved, and the larger the longitudinal tube spacing of the oval-tube is, the smaller the influence on the comprehensive performance of the recuperator is.

4. ANALYSIS OF ENHANCED HEAT TRANSFER MECHANISM

4.1 Shell side flow field distribution

When the fluid flows through the oval tube, the position, velocity, temperature and pressure change violently before and after the oval tube. The front and rear segments of the second oval tube of the recuperator model are selected for specific analysis, and the position diagram is shown in Fig. 9.

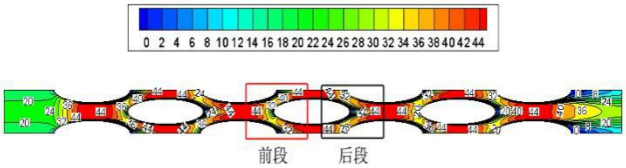

Fig. 9 schematic diagram of an oval-tube recuperator

4.1.1 Flow condition

The front and back sections of the oval-tube are taken respectively, and the velocity, temperature and pressure distribution of the fluid in the recuperator shell under different Reynolds numbers are analyzed. The obtained contour clouds are shown in Fig.10

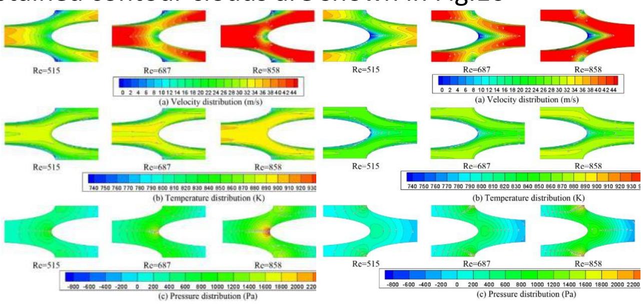

Fig. 10 Distribution of flow field for different Reynolds number

When Reynolds number is 687, the maximum velocity and fluid temperature appear at the short axis of oval-tube, and the minimum value of velocity and pressure is at the long axis of oval-tube. With the increase of Reynolds number, the velocity gradient and pressure gradient become steeper, and the fluid temperature in the same position increases.

4.1.2 Structural parameters

The front and back segments of the intermediate oval-tube are intercepted respectively, and the velocity, temperature and pressure distribution of the fluid in the shell side of the recuperator under four structural parameters are compared and analyzed. The obtained contour clouds are shown in Fig. 11.

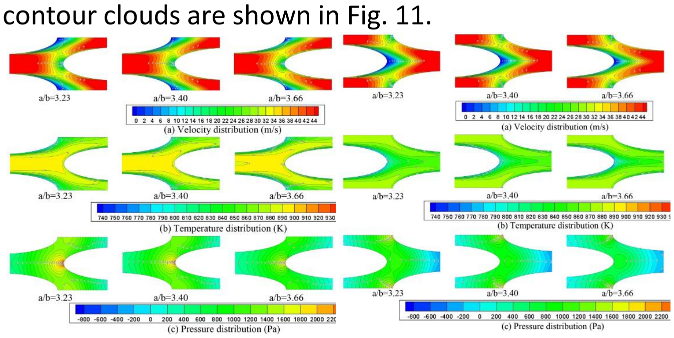

Fig. 11 Distribution of flow field for different structural parameters

When the structural parameter *a/b*=3.40, the maximum value of the flow rate appears at the minor axis of the elliptic tube, and the minimum value of the fluid velocity, pressure and temperature appears at the long axis of the elliptic tube, and the fluid temperature gradually rises and the fluid pressure is gradually decreased along the fluid flow direction; As the structural parameter *a/b* increases, the velocity at the same position increases, the lower the temperature of the fluid at the same position, the velocity gradient becomes steeper, and the pressure gradient becomes slower.

4.1.3 Tube arrangement mode

The front and back segments of the middle oval-tube are intercepted respectively, and the velocity, temperature and pressure distribution of the fluid in the shell side of the recuperator with four kinds of transverse tube spacing and longitudinal spacing are compared and analyzed. The obtained contour clouds are shown in Figs.12 and 13.

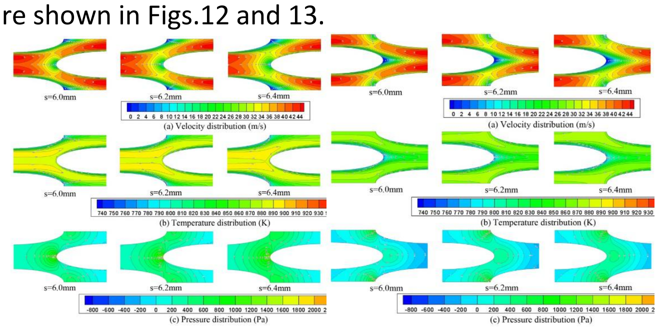

Fig.12 Distribution of flow field for different transverse tube spacing

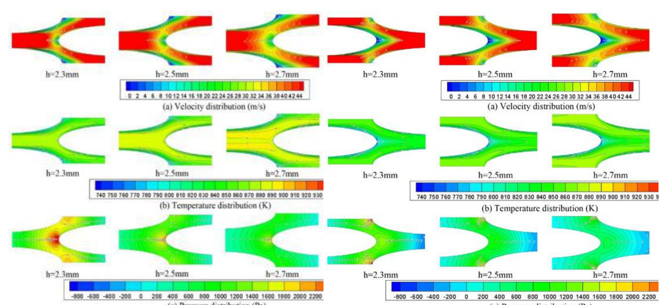

Fig.13 Distribution of flow field for different longitudinal tube spacing

When the transverse tube spacing is *s*=6.2mm, the maximum velocity appears at the short shaft of the oval-tube, and the minimum value of fluid velocity, temperature and pressure appears at the long axis of the oval-tube. The larger the transverse tube spacing is, the slower the velocity gradient and pressure gradient are. The higher the fluid temperature in the same position, the better the heat transfer effect. When the longitudinal tube spacing is *h*=2.5mm, the maximum velocity appears at the short shaft of the oval-tube, and the minimum value of fluid velocity and temperature pressure appears at the long axis of the oval-tube. The larger the longitudinal tube spacing h is, the slower the velocity gradient and pressure gradient are, and the higher the fluid temperature in the same position is.

4.2 Field coordination principle

In order to analyze the enhanced heat transfer mechanism of the shell side fluid flow and heat transfer of the oval tube reheater, the velocity field and temperature field of the recuperator shell are calculated by using the principle of field synergy[9]. The calculated results are shown in Fig. 14. It can be seen from the figure that in the inlet section of the recuperator, the angle between the velocity vector and the temperature vector varies slightly in a certain range, and in the inner part of the recuperator, the fluctuation range of the synergy angle is large and shows a certain periodicity.

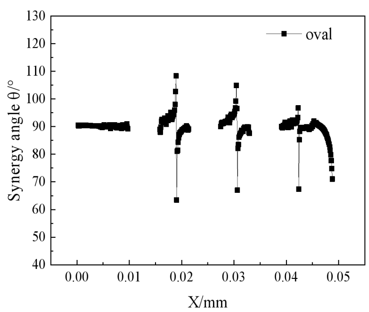

Fig.14 Synergetic angular distribution diagram

5. CONCLUSIONS

In this study, the shell heat transfer and resistance performance of oval-tube recuperator and its influencing factors are studied by numerical simulation method, and the heat transfer enhancement mechanism of the recuperator is discussed, including the following contents:

(1) Compared with the experimental results, the standard *k-ε* turbulence model is much more feasible and accurate than others. Based on this, an accurate CFD numerical model and method of this new combined separator are proposed.

(2) Heat transfer and resistance characteristics: The heat transfer and resistance performance increase with the ratio of major and minor axes and longitudinal spacing of oval-tube. With the increase of horizontal and longitudinal spacing of oval-tube, the performance increases at first and then decreases.

(3)Flow field characteristics and field synergy principle: The maximum velocity appears at the minor axis, and the minimum value of fluid temperature, velocity and pressure appears at the major axis. The amplitude of field synergy angle is small in the inlet section, but the fluctuation amplitude in the recuperator is large.

REFERENCE

[1] John Leahy. Delivering the future global market forecast.2011-2030[R]. Blagnac: Airbus, 2011.

[2] Harald Schoenenborn, Ernst Ebert, Burkhard Simon, et al. Thermomechanical design of a Heat Exchanger for a Recuperative Aeroengine[J]. Journal of Engineering for Gas Turbines and Power. 2006, 128: 736-744.

[3] June Kee Min, Ji Hwan Jeong, Man Yeong Ha, et al. High temperature heat exchanger studies for applications to gas turbines[J]. Heat Mass Transfer. 2009, 46(10): 175-186.

[4] Kritikos K, Albanakis C, Missirlis D, et al. Investigation of the thermal efficiency of a staggered elliptic-tube heat exchanger for aeroengine applications[J]. Applied Thermal Engineering. 2010, 30(2): 134-142.

[5] Kyprianidis K G, Grönstedt T, Ogaji S O, et al. Assessment of Future Aero-engine Designs With Intercooled and Intercooled Recuperated Cores[J]. Journal of Engineering for Gas Turbines & Power. 2010, 133(1): 01170101-01170110.

[6] Bouris D, Kubo R, Hirata H, et al. Numerical Comparative Study of Compressor Rotor and Stator Blade Deposition Rates[J]. Journal of Engineering for Gas Turbines & Power. 2002, 124(3): 608-616.

[7] Tao WQ. Numerical heat transfer (second edition) [M]. Xi'an: Xi'an Jiaotong University Press, 2001.(in Chinese)

[8] Goulas A, Donnerhack S, Flouros M, et al. Thermodynamics Cycle Analysis, Pressure Loss, and Heat Transfer Assessment of a Recuperative System for Aero-Engines[J]. Journal of Engineering for Gas Turbines and Power. 2018, 137(4): 1-6.

[9] Guo ZY. Field synergy principle in regenerator and its application [J]. Journal of Mechanical Engineering. 2003, 39 (12): 1-9.(in Chinese)